Evaluating Snow Bidirectional Reflectance of Models Using Multiangle Remote Sensing Data and Field Measurements

Lizao Ye, Pengfeng Xiao, *Senior Member, IEEE*, Xueliang Zhang, *Member, IEEE*, Xuezhi Feng, Rui Hu, Wei Ma, Haixing Li, Yina Song, and Tengyao Ma

***Abstract*— Because of the anisotropy of snow surface reflectance, it is essential to select a proper snow bidirectional reflectance model for extracting snow cover and inverting snow properties from remote sensing image, especially during the period of snow rapidly changed. In this letter, the ability of reproducing snow bidirectional reflectance by three semiempirical bidirectional reflectance distribution function (BRDF) models (Ross–Li, Roujean, and Raman–Pinty–Verstraete) and the asymptotic radiative transfer theory (ART) model was evaluated using the polarization and directionality of the earth reflectance (POLDER) data. In addition, the ART model was compared with the bicontinuous geometric optics (bic-GORT) model based on field measurements. The results indicated that the root mean square errors (RMSEs) are small and similar for all models during the stable-snow period. The physical models perform better than the semiempirical models in capturing the bidirectional signatures of snow during the periods of snow rapidly changed. The bic-GORT model achieves higher accuracy, while the ART model holds the advantages of simple and efficient to be used.**

***Index Terms*— Bidirectional reflectance distribution function (BRDF) model, evaluation, polarization and directionality of the earth reflectance (POLDER), remote sensing, snow.**

I. Introduction

SEASONAL snow is an important part of the cryosphere and a sensitive indicator of global climate change [1], [2]. Remote sensing is able to monitor snow cover in a wide range. Considering the anisotropy of snow surface reflectance, it is necessary to make use of a bidirectional reflectance distribution function (BRDF) model to correct the anisotropic effect for extracting snow cover [3] and inverting snow properties, e.g., albedo [4], snow grain size, and pollutants [5].

The BRDF models can be classified into empirical, semiempirical, and physical (or radiative transfer) models [6]. The semiempirical models are widely used for producing reflectance or albedo products (including snow cover). For example, the Ross–Li model was successfully used to produce Moderate Resolution Imaging Spectroradiometer (MODIS) BRDF/albedo products [4] and Nadir BRDF-Adjusted Reflectance [7]. The Roujean model [8] and the Raman–Pinty–Verstraete (RPV) model [9] were developed for correcting surface bidirectional effect in time series of satellite observations. Although the semiempirical models were not built explicitly for snow surfaces, they can seize the geometric-optical effect caused by the shadowing of rugged or undulating snow surface [10]. As usual, the kernels of the semiempirical models can be simplified from the physical models, but the estimation of model parameters requires many observations with different view angles [11]. Generally, the satellites (such as MODIS, Landsat, and Sentinel-2) only provide reflectance value at a specific view zenith angle. This means that multiday observations are needed to obtain the multiangle reflectance for snow surface. Therefore, when using the semiempirical models, we need to ignore the change of snow's anisotropy characteristics within a period of multiple observations. However, the characteristics of snow change rapidly (e.g., during the periods of ablation or accumulation), which may bring uncertainties for estimating snow properties by using the semiempirical models.

Several physical models of snow BRDF have been developed and validated with field measurements [12]. The Wiscombe and Warren (WW) model could accurately estimate the change of directional-hemispherical albedo with solar zenith angle [13], but it could not reproduce the BRDF trait of snow [14]. The discrete ordinates radiative transfer (DISORT) model [15] was proposed to simulate the BRDF characteristics of snow under the assumption of spherical snow particles [16], but it was limited in describing the anisotropy of snow using the radiative transfer models of spherical snow particles at large view zenith angle [17]. The geometric optics theory was used to solve the single-scattering characteristics of the bicontinuous medium of snow microstructure [referred as bicontinuous geometric optics (bic-GORT) model], which can simulate the directional reflection of pure and flat snow [18].

The asymptotic radiative transfer theory (ART) model was developed based on the semiinfinite and weak absorption medium of snow [19]. The assumption of fractal snow grain is closer to real snow than the assumption of spherical snow grain. After a series of improvements, the ART model comprehensively considered the influence of snow grain size and pollutant on the directional reflection characteristics of

Manuscript received April 7, 2020; revised July 22, 2020; accepted September 15, 2020. Date of publication September 29, 2020; date of current version December 16, 2021. This work was supported in part by the Science and Technology Basic Resources Investigation Program of China under Grant 2017FY100502 and in part by the National Natural Science Foundation of China under Grant 41671344 *(Corresponding authors: Pengfeng Xiao; Xueliang Zhang.)*

Lizao Ye, Pengfeng Xiao, Xueliang Zhang, Xuezhi Feng, Rui Hu, Wei Ma, Yina Song, and Tengyao Ma are with the Jiangsu Provincial Key Laboratory of Geographic Information Science and Technology, Key Laboratory for Land Satellite Remote Sensing Applications of Ministry of Natural Resources, School of Geography and Ocean Science, Nanjing University, Nanjing 210023, China (e-mail: xiaopf@nju.edu.cn; zxl@nju.edu.cn).

Haixing Li is with the College of Geomatics Science and Technology, Nanjing Tech University, Nanjing 211816, China.

Digital Object Identifier 10.1109/LGRS.2020.3024731

snow [20], [21], and was used to retrieve snow albedo, grain size, and absorption coefficient of pollutants [22], [23], showing a great potential to be used for snow in terms of both simulating and retrieving snow properties.

In this letter, we aim at comparing the performance of three widely used semiempirical BRDF models (i.e., Ross–Li, Roujean, and RPV) with the ART model on reproducing multiangle reflectance of snow based on the polarization and directionality of the earth reflectance (POLDER) data, especially during the period of snow morphology changed rapidly. In addition, the physical models ART and bic-GORT were compared with each other based on field measurements. These comparison results could help users to understand both the advantages and limitations of different models for different snow status [6], [20].

The rest of this letter is organized as follows. The five involved BRDF models are briefly introduced in Section II. The POLDER and field measurement data are presented in Section III. The evaluation method and results are described in Sections IV and V, respectively. The discussions and conclusions are made in Sections VI and VII, respectively.

II. BRDF Models

Five widely used BRDF models are compared in this study, including the linear kernel-driven models Ross–Li and Roujean, the nonlinear semiempirical model RPV, and the physical models ART and bic-GORT.

A. Linear Kernel-Driven Models

The Ross–Li model is a classical linear kernel-driven model used to produce MODIS BRDF/albedo products [4]. It is described as the weighted summation of an isotropic parameter and two kernel functions where the volume scatter kernel is derived from the volume-scattering radiative transfer model [24] and the geometry optical kernel is derived from the surface scattering and geometric shadow casting theory [25].

The Roujean model [8] has the same volume scatter kernel as the Ross–Li model but a different geometry optical kernel, which can reduce the bidirectional effects of multitemporal remote sensing data [6]. The two linear kernel-driven models have three parameters that need to be estimated from observations.

B. RPV Model

The RPV model [9] is a nonlinear semiempirical model describing the bidirectional reflectance of natural surfaces. It is derived from both physical and geometrical considerations of radiation transfer through a porous medium. The RPV model can be used to generate theoretical bidirectional reflectance, and thus to quantitatively analyze the surface bidirectional reflectance using remote sensing data [26]. The RPV model also has three parameters.

C. ART Model

The ART model assumes snow layer as a semiinfinite and weak absorption medium. The single-scattering property of the particles is calculated by the geometrical optics method, and the asymptotic solution is obtained by the asymptotic radiation transfer theory [27]. The ART model has two parameters: effective optical grain size and pollutant [20]. The value of pollutant is proportional to the imaginary part of the refractive index of pollutants, which depends on the wavelength [28], [29]. The effective optical grain size can be retrieved from sensitive spectral bands, e.g., 1020 nm [20], [30].

D. Bic-GORT Model

In the bic-GORT model, the bicontinuous medium is used to simulate the snow microstructure, considering its randomness and complexity. The geometric optics theory is used to simulate the scattering of snow [18]. The model is able to simulate the albedo, multiangle reflectance, polarized reflectance, and the specific surface area of snow [31], [32].

The parameters of the semiempirical models need to be estimated using multiangle reflectance data obtained by remote sensing or field measurements. It requires that the data cover angles as wide as possible. However, the parameters of the ART model could be retrieved from reflectance by the model itself [20], [28]–[30], and the parameters of the bic-GORT model can be obtained by field measurements [18], [31], [32].

III. Data

The multiangle reflectance of snow obtained by POLDER-3 was used for evaluating the semiempirical models and the ART model. The multiangle data were obtained by overlapping the field of view of the sensor. Each pixel was observed at a maximum of 16 (average is 14) different view angles during a single transit of the satellite. The view zenith angle along orbit direction can reach $\pm 61°$, and the view zenith angle perpendicular to the orbit direction can reach $\pm 50°$ [32]. The POLDER-3 data passed the cloud detection for each month (https://doi.pangaea.de/10.1594/PANGAEA.864090), in which the reflectance of snow was specifically used [33]. We chose the multiangle reflectance of snow pixel with homogeneity $=$ 100% and blue band (490 nm) reflectance > 0.4 to make sure that the multiangle reflectance was collected from snow surface [26]. Accordingly, the data from February to October 2008 in the Arctic were selected.

Since the parameters of the bic-GORT model, such as snow depth, density, and effective optical grain size, cannot be obtained through the POLDER-3 data, the field measurement data were used for evaluating the bic-GORT model and the ART model. The field measurement was implemented over a flat snow surface after a snowfall on April 12, 2018 in Tianshan Mountains, northwestern China. The snow multiangle reflectance was measured by the ASD FieldSpec-3 spectroradiometer. The relative view azimuth angles include 0°, 45°, 90°, 135°, 180°, 225°, 270°, and 315° from the principal plane. For each view azimuth angle, the reflectance was measured at the view zenith angle range from 0° (the nadir) to 70° with a resolution of 10°. In addition, we measured the snow depth, density, and effective optical grain size, which can be used for running the bic-GORT model.

Snow shows an obvious anisotropy at the near-infrared bands, and tends to be isotropic at visible bands [34]. Thus, we selected the near-infrared bands to evaluate the ability of capturing the snow bidirectional signatures for different models including wavelengths 765, 865, and 1020 nm.

IV. Methodology

For the three semiempirical models, the parameters were, respectively, estimated by the multiangle reflectance data

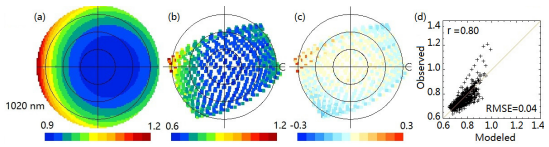

Fig. 1. Example of the comparison of the multiangle reflectance reproduced by (a) ART model and (b) POLDER data, where the constant viewing zenith angles are represented as circles every 20° and the principal plane is on the horizontal straight line with backscattering to the right. (c) and (d) AEs and scatter plot of the modeled and measured reflectance, respectively.

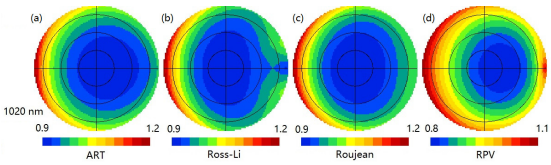

Fig. 2. Example of the comparison of the multiangle reflectance reproduced by the ART model (a) and the semiempirical models (b)–(d) based on the POLDER data.

obtained by the POLDER through minimizing the root mean square error (RMSE) [6]. For the ART model, the effective optical grain size was retrieved from the reflectance at the wavelength of 1020 nm [20]. For the bic-GORT model, the snow depth, density, and observation geometry conditions were obtained by field measurements, and the other parameters were set as the default values. The RMSE, Pearson correlation coefficient (r), and absolute error (AE) between the modeled and observed multiangle reflectance were calculated for comparing the BRDF models [6].

V. Results

A. Model Evaluation Based on POLDER Data

Fig. 1 shows an example of comparing the multiangle reflectance reproduced by the ART model with the POLDER data. It is shown that the shape of the snow BRDF likes a bowl. The snow reflectance is small in the center of the circle, whereas it is large in the outside of the circle, especially in the forward detection at the solar principal plane. The AE between the multiangle reflectance reproduced by the ART model and the POLDER data ranges from −0.3 to 0.3. The large AE mainly occurs at a large view zenith angle. At the solar principal plane, the multiangle reflectance reproduced by the ART model is smaller than that of the POLDER data in forward direction, but it is greater in backward direction. The AE is small at the small view zenith or at the perpendicular principal plane of the solar. The RMSE at the wavelength of 1020 nm is 0.04, and r is 0.80.

Fig. 2 shows an example of the multiangle reflectance of snow reproduced by the ART model and the semiempirical models based on the POLDER data. These models can effectively reproduce the bowl-like shape of the snow BRDF. They both reflect the strong forward radiation characteristics of snow surface, but present differences in the back radiation. Specially, there is a valley value at backward direction reproduced by the Ross–Li model, but it has a peak value by the RPV model. The reason is that the Ross–Li model has a theoretical valley value in the backward direction. By contrast, the RPV model enlarges the backscattering, thus it has a peak value in the backward direction. Nevertheless, there is no obvious valley

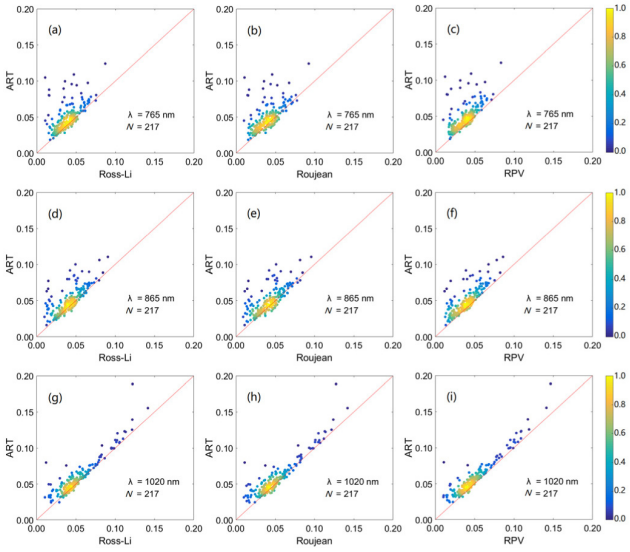

Fig. 3. Comparison of the RMSEs of different BRDF models. (a)–(c), (d)–(f), and (g)–(i) Comparison of the RMSEs of the ART and the semiempirical models at 765, 865, and 1020 nm, respectively. N is the number of observations.

or peak value of multiangle reflectance reproduced by the ART and the Roujean model in the backward direction.

Fig. 3 shows the RMSEs of the multiangle reflectance reproduced by different models with reference to the POLDER data. The RMSEs are centralized on 0.05 for all the models. The number of points with RMSE difference less than 0.1 accounts for 97% at the wavelength of 1020 nm, and even reaches 99% for other wavelengths, showing that all the models hold the ability to capture the bidirectional characteristics of snow.

B. Model Evaluation on Sites With Large RMSEs

Among the results in Section V-A, we found two sites with ART RMSEs greater than 0.15 at 1020 nm, where one RMSE is 0.19, and the other is 0.16. The first site is located in Iceland with the POLDER data collected in September 2008. The second site is located in Canada with the POLDER data collected in June 2008. The reasons for the large ART RMSEs are explored as follows.

The site located in Iceland with the largest RMSE of 0.19 is investigated in Fig. 4. The snow reflectance could be apparently separated into two groups. One group was collected on September 3, and the other was collected on September 23 and 30. The reflectance at 1020 nm was ranging from 0.35 to 0.45 and from 0.60 to 0.90 in the two groups, respectively, indicating that the morphology of snow changed apparently during September. The retrieved effective optical grain size based on the aggregated reflectance could not represent all the different grain sizes in September because the snow morphology changed rapidly, which results in the large RMSE of this site. However, after separating the data into two groups, the RMSE of the ART model decreases to 0.02 as shown in Fig. 4, demonstrating the effectiveness of the ART model on dealing with rapidly changed snow.

In order to further illustrate the influence of rapidly changed snow morphology, the RMSEs of the semiempirical and the ART models at the wavelength of 1020 nm in the two sites

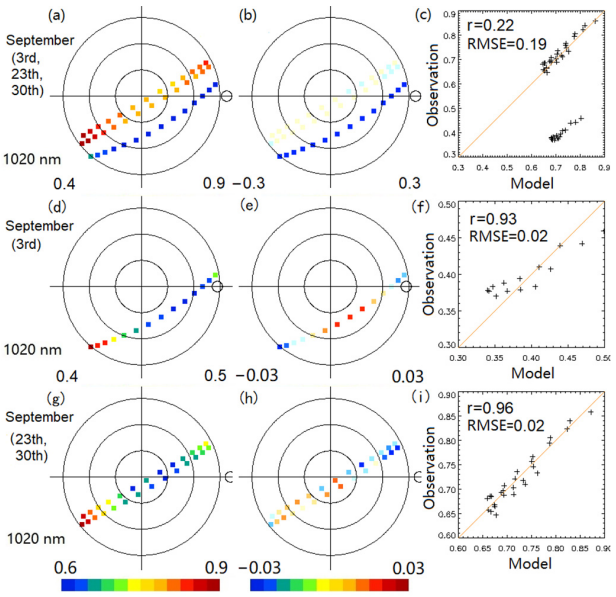

Fig. 4. Details of the site with the largest RMSE. (a), (d), and (g) are observed data in September. (b), (e), and (h) are AEs of the ART modeled and measured reflectance. (c), (f), and (i) are scatter plots of the ART modeled and measured reflectance.

TABLE I
RMSEs OF THE SEMIEMPIRICAL AND THE ART MODELS AT 1020 nm

Observation	Ross-Li	Roujean	RPV	ART
September aggregated	0.12	0.13	0.15	0.19
3 September				0.02
23 and 30 September				0.02
June aggregated	0.14	0.14	0.14	0.16
Before 23 June				0.06
After 24 June				0.04

are shown in Table I. The snow reflectance of the site located in Canada was also separated into two groups based on the reflectance difference caused by snow morphology change. One group of snow reflectance was collected before June 23, and the other group was collected after June 24. Table I shows that both the semiempirical and the ART models have high RMSEs when aggregating the three observations, i.e., they are negatively influenced by the snow morphology changes when using the multiday satellite images. The ART model would have larger RMSE because of the sensitivity to effective optical grain size. During an observed circle with snow morphology change, one retrieved effective optical grain size could not represent all the effective optical grain size. However, after separating the observed circle into groups in which the snow morphology does not change significantly, the RMSE of the ART model decreases apparently and becomes much lower than the semiempirical models. These results further demonstrate that the ART model holds the advantage of overcoming the problem of snow morphology change without dependence on multiple observations.

C. Physical Model Evaluation Based on Field Measurements

The physical models ART and bic-GORT were evaluated based on the field-measured multiangle reflectance of snow. The RMSEs of the ART and the bic-GORT model are both small as shown in Table II. The bic-GORT model has relatively lower RMSEs than the ART model at the three wavelengths. The reason may be that the bicontinuous medium adopted by the bic-GORT model is closer to the real snow microstructure.

TABLE II
RMSEs OF THE ART AND THE BIC-GORT MODELS

Model	765 nm	865 nm	1020 nm
ART	0.088	0.083	0.074
bic-GORT	0.051	0.049	0.045

VI. DISCUSSION

A. Advantages of the ART Model

The parameters of the ART model have physical significance and can be applied to all bands (the pollutant even can be ignored at the long wavelength bands), while the parameters of semiempirical models do not have physical significance and need to be estimated from multiangle reflectance. The parameters of the semiempirical models are different for different spectral bands, which increases the computational complexity and is not conducive to generalization. When we use the semiempirical models, we need to ignore the changes of snow's anisotropy caused by the changed snow morphology within a period of multidays. However, the physical models simulate the multiangle reflectance conveniently without the dependence on multiday observations. Comparing the ART model with the bic-GORT model, the latter has more parameters that are demanding to be obtained. However, the two parameters of the ART model can be retrieved from the reflectance at a sensitive wavelength, which makes the ART model simple and efficient to be used.

B. Limitation of the ART Model

The pollutant of the ART model is proportional to the imaginary part of the refractive index of pollutants [28], which cannot meet the different properties of snow. The ART model is sensitive to the absorption coefficient at the short wavelength. Therefore, we can find that the RMSEs of the ART model are slightly greater than that of the semiempirical models at short wavelength in Fig. 3. Furthermore, the specular light reflection by partially oriented snow plates on the snow surface is not considered by the ART model, which can play a role for measurements in the principal plane [27]. Therefore, the AEs are large in the forward direction in the solar principal plane. The bic-GORT model uses the bicontinuous medium that is closer to the microstructure of actual snow than the ART model, which may be the reason that the accuracy of the ART model is not as high as the bic-GORT model in the evaluation results.

C. Influence of the Change of Snow Morphology

When the snow morphology changes rapidly, such as during the periods of ablation and accumulation, the snow's anisotropy changes significantly. The semiempirical models require multiangle reflectance to estimate the parameters. Generally, satellites (such as MODIS, Landsat, and Sentinel-2) only provide reflectance value at a specific view zenith angle by one observation. This means that multiday observations are needed to obtain the multiangle reflectance of snow surface.

The performance of the semiempirical models would thus be negatively influenced by using the multiday satellite images. In this case, the physical models such as the ART shows the advantage to overcome the problem of snow morphology change by obtaining the parameters from a single observation. These are very important for extracting snow cover and retrieving snow properties by using remote sensing data when snow morphology changes rapidly.

VII. Conclusion

We adopted the POLDER-3 and field measurement data to evaluate the ability of the five BRDF models on capturing the bidirectional signature of snow surface, especially for snow with rapidly changed morphology. The following conclusions can be obtained through the results and discussions: 1) the accuracies of the five BRDF models are high and similar during the stable-snow period; 2) the physical model performs better than the semiempirical models during the periods of snow rapidly changed without the dependence on multiple observations for estimating the parameters; and 3) the bic-GORT model achieves higher accuracy than the ART model, while the ART model holds the advantage of simple and efficient to be used by obtaining the parameters more easily.

References

[1] J. Dozier, R. O. Green, A. W. Nolin, and T. H. Painter, "Interpretation of snow properties from imaging spectrometry," *Remote Sens. Environ.*, vol. 113, pp. S25–S37, Sep. 2009.

[2] T. Aoki, T. Aoki, M. Fukabori, A. Hachikubo, Y. Tachibana, and F. Nishio, "Effects of snow physical parameters on spectral albedo and bidirectional reflectance of snow surface," *J. Geophys. Res., Atmos.*, vol. 105, no. D8, pp. 10219–10236, Apr. 2000.

[3] M. Salminen, J. Pulliainen, S. Metsämäki, J. Ikonen, K. Heinilä, and K. Luojus, "Determination of uncertainty characteristics for the satellite data-based estimation of fractional snow cover," *Remote Sens. Environ.*, vol. 212, pp. 103–113, Jun. 2018.

[4] C. Schaaf *et al.*, "First operational BRDF, Albedo Nadir reflectance products from MODIS," *Remote Sens. Environ.*, vol. 83, no. 1, pp. 135–148, 2002.

[5] E. P. Zege, I. L. Katsev, A. V. Malinka, A. S. Prikhach, G. Heygster, and H. Wiebe, "Algorithm for retrieval of the effective snow grain size and pollution amount from satellite measurements," *Remote Sens. Environ.*, vol. 115, no. 10, pp. 2674–2685, Oct. 2011.

[6] F. Maignan, F.-M. Bréon, and R. Lacaze, "Bidirectional reflectance of Earth targets: Evaluation of analytical models using a large set of spaceborne measurements with emphasis on the hot spot," *Remote Sens. Environ.*, vol. 90, no. 2, pp. 210–220, Mar. 2004.

[7] Z. Wang, C. B. Schaaf, Q. Sun, Y. Shuai, and M. O. Román, "Capturing rapid land surface dynamics with collection V006 MODIS BRDF/NBAR/albedo (MCD43) products," *Remote Sens. Environ.*, vol. 207, pp. 50–64, Mar. 2018.

[8] J.-L. Roujean, M. Leroy, and P.-Y. Deschamps, "A bidirectional reflectance model of the Earth's surface for the correction of remote sensing data," *J. Geophys. Res., Atmos.*, vol. 97, no. D18, pp. 20455–20468, 1992.

[9] H. Rahman, B. Pinty, and M. M. Verstraete, "Coupled surface-atmosphere reflectance (CSAR) model: 2. Semiempirical surface model usable with NOAA advanced very high resolution radiometer data," *J. Geophys. Res.*, vol. 98, no. D11, p. 20791, 1993.

[10] Z. Jiao *et al.*, "Development of a snow kernel to better model the anisotropic reflectance of pure snow in a kernel-driven BRDF model framework," *Remote Sens. Environ.*, vol. 221, pp. 198–209, Feb. 2019.

[11] W. Lucht, C. B. Schaaf, and A. H. Strahler, "An algorithm for the retrieval of albedo from space using semiempirical BRDF models," *IEEE Trans. Geosci. Remote Sens.*, vol. 38, no. 2, pp. 977–998, Mar. 2000.

[12] T. H. Painter and J. Dozier, "Measurements of the hemispherical-directional reflectance of snow at fine spectral and angular resolution," *J. Geophys. Res.*, vol. 109, no. D18, pp. 1–21, 2004.

[13] W. J. Wiscombe and S. G. Warren, "A model for the spectral albedo of snow. I: Pure snow," *J. Atmos. Sci.*, vol. 37, no. 12, pp. 2712–2733, Dec. 1980.

[14] A. W. Nolin and S. Liang, "Progress in bidirectional reflectance modeling and applications for surface particulate media: Snow and soils," *Remote Sens. Rev.*, vol. 18, nos. 2–4, pp. 307–342, Sep. 2000.

[15] K. Stamnes, S.-C. Tsay, W. Wiscombe, and K. Jayaweera, "Numerically stable algorithm for discrete-ordinate-method radiative transfer in multiple scattering and emitting layered media," *Appl. Opt.*, vol. 27, no. 12, pp. 2502–2509, 1988.

[16] T. H. Painter and J. Dozier, "The effect of anisotropic reflectance on imaging spectroscopy of snow properties," *Remote Sens. Environ.*, vol. 89, no. 4, pp. 409–422, Feb. 2004.

[17] M. Mishchenko *et al.*, "Bidirectional reflectance of flat, optically thick particulate layers: An efficient radiative transfer solution and applications to snow and soil surfaces," *J. Quant. Spectrosc. Radiat.*, vol. 63, no. 2, pp. 409–432, 1999.

[18] C. Xiong, J. Shi, D. Ji, T. Wang, Y. Xu, and T. Zhao, "A new hybrid snow light scattering model based on geometric optics theory and vector radiative transfer theory," *IEEE Trans. Geosci. Remote Sens.*, vol. 53, no. 9, pp. 4862–4875, Sep. 2015.

[19] A. A. Kokhanovsky and E. P. Zege, "Scattering optics of snow," *Appl. Opt.*, vol. 43, no. 7, pp. 1589–1602, 2004.

[20] A. A. Kokhanovsky and F.-M. Breon, "Validation of an analytical snow BRDF model using PARASOL multi-angular and multispectral observations," *IEEE Geosci. Remote Sens. Lett.*, vol. 9, no. 5, pp. 928–932, Sep. 2012.

[21] H. Wiebe, G. Heygster, E. Zege, T. Aoki, and M. Hori, "Snow grain size retrieval SGSP from optical satellite data: Validation with ground measurements and detection of snow fall events," *Remote Sens. Environ.*, vol. 128, pp. 11–20, Jan. 2013.

[22] J. Wang, X. Feng, P. Xiao, N. Ye, X. Zhang, and Y. Cheng, "Snow grain-size estimation over mountainous areas from MODIS imagery," *IEEE Geosci. Remote Sci.*, vol. 15, no. 1, pp. 97–101, Jan. 2018.

[23] A. Kokhanovsky *et al.*, "The determination of snow albedo from satellite measurements using fast atmospheric correction technique," *Remote Sens.*, vol. 12, no. 2, p. 234, Jan. 2020.

[24] J. Ross, *The Radiation Regime and Architecture of Plant Stands*. The Hague, The Netherlands: Dr. W. W. Junk, 1981.

[25] X. Li and A. H. Strahler, "Geometric-optical bidirectional reflectance modeling of the discrete crown vegetation canopy: Effect of crown shape and mutual shadowing," *IEEE Trans. Geosci. Remote Sens.*, vol. 30, no. 2, pp. 276–292, Mar. 1992.

[26] Y. Qu, Q. Liu, S. Liang, L. Wang, N. Liu, and S. Liu, "Direct-estimation algorithm for mapping daily land-surface broadband albedo from MODIS data," *IEEE Trans. Geosci. Remote Sens.*, vol. 52, no. 2, pp. 907–919, Feb. 2014.

[27] A. A. Kokhanovsky, T. Aoki, A. Hachikubo, M. Hori, and E. P. Zege, "Reflective properties of natural snow: Approximate asymptotic theory versus *in situ* measurements," *IEEE Trans. Geosci. Remote Sens.*, vol. 43, no. 7, pp. 1529–1535, Jul. 2005.

[28] A. Kokhanovsky *et al.*, "Sizing snow grains using backscattered solar light," *Int. J. Remote Sens.*, vol. 32, no. 22, pp. 6975–7008, Nov. 2011.

[29] A. Kokhanovsky *et al.*, "Retrieval of snow properties from the Sentinel-3 ocean and land colour instrument," *Remote Sens.*, vol. 11, no. 19, p. 2280, Sep. 2019.

[30] A. Kokhanovsky *et al.*, "On the reflectance spectroscopy of snow," *Cryosphere*, vol. 12, no. 7, pp. 2371–2382, Jul. 2018.

[31] C. Xiong and J. Shi, "Snow specific surface area remote sensing retrieval using a microstructure based reflectance model," *Remote Sens. Environ.*, vol. 204, pp. 838–849, Jan. 2018.

[32] A. Ding *et al.*, "An assessment of the performance of two snow kernels in characterizing snow scattering properties," *Int. J. Remote Sens.*, vol. 40, no. 16, pp. 6315–6335, Aug. 2019.

[33] F.-M. Breon and F. Maignan, "A BRDF–BPDF database for the analysis of Earth target reflectances," *Earth Syst. Sci. Data*, vol. 9, no. 1, pp. 31–45, Jan. 2017.

[34] S. R. Hudson, S. G. Warren, R. E. Brandt, T. C. Grenfell, and D. Six, "Spectral bidirectional reflectance of antarctic snow: Measurements and parameterization," *J. Geophys. Res.*, vol. 111, no. D18, 2006.